NJC

PAPER

View Article Online
View Journal

Cite this: DOI: 10.1039/c5nj00939a

Highly efficient yellow phosphorescent OLEDs based on two novel bipolar host materials†

Song Zhang, Qiu-Lei Xu, Jing-Cheng Xia, Yi-Ming Jing, You-Xuan Zheng* and Jing-Lin Zuo

Received (in Montpellier, France)
15th April 2015,
Accepted 27th July 2015

DOI: 10.1039/c5nj00939a

www.rsc.org/njc

Two bipolar host materials, N^1-(naphthalen-1-yl)-N^1,N^4-diphenyl-N^4-(4-(5-phenyl-1,3,4-oxadiazol-2-yl)phenyl)naphthalene-1,4-diamine (**NONP**) and N^1-(naphthalen-1-yl)-N^1,N^4-diphenyl-N^4-(3-(5-phenyl-1,3,4-oxadiazol-2-yl)phenyl)naphthalene-1,4-diamine (**NONM**), comprising a hole-transporting N^1-(naphthalen-1-yl)-N^1,N^4-diphenylnaphthalene-1,4-diamine (**NPNA2**) donor and an electron-transporting 1,3,4-oxadiazole (**OXD**) acceptor at different phenyl bridge positions, have been synthesized. **NONP** (glass transition temperature T_g = 127 °C) and **NONM** (T_g = 105 °C) exhibit high morphological stability. The theoretical calculations on both hosts show that the HOMOs (highest occupied molecular orbitals) are mainly dispersed on the electron-donating groups, and the LUMOs (lowest unoccupied molecular orbitals) are predominantly dispersed on the electron-accepting units, suggesting bipolar charge transporting property. Two yellow phosphorescent organic light-emitting diodes (PHOLEDs, ITO (indium tin oxide)/TAPC (1,1-bis[4-(di-*p*-tolylamino) phenyl]cyclohexane, 40 nm)/host: Ir(bt)$_2$(acac) (bis(2-phenylbenzothiozolato-*N*,$C^{2\prime}$) iridium(acetylacetonate), 15 wt%, 20 nm)/TmPyPB (1,3,5-tri(*m*-pyrid-3-yl-phenyl) benzene, 40 nm)/LiF (1 nm)/Al (100 nm)) fabricated using **NONP** and **NONM** as the host and Ir(bt)$_2$(acac) as the emitter exhibit maximum current efficiencies ($\eta_{c,max}$) of 43.2 and 44.4 cd A^{-1}, respectively, with low current efficiency roll-off. The values of 40.4 and 43.6 cd A^{-1} can still be achieved at the luminance of 3000 cd m^{-2}, respectively.

Introduction

In the last few years, the organic light-emitting diode (OLEDs) industry has enjoyed fast growth, as OLEDs are widely considered to be the leading next-generation display and lighting technology. Among these devices, tremendous efforts have been made to improve the phosphorescent organic light-emitting diodes (PHOLEDs) because they can reach 100% internal quantum efficiency by harvesting both electro-generated singlet and triplet excitons for emission.[1] The emissive layer of a PHOLED is usually doped with an organometallic complex, which contains heavy metal atoms (usually iridium). The interaction between the heavy metal and organic molecules can result in more efficient emitters with longer lifetime. However, the emission lifetime and high concentration of these heavy metal complexes easily lead to undesired efficiency roll-off at high current density during the operation of a device.[2] Therefore, to achieve highly efficient electrophosphorescence by reducing competitive factors such as concentration quenching and triplet–triplet annihilation, phosphorescent emitters of heavy-metal complexes are usually doped uniformly in an organic host material.[3] The design of appropriate host materials is of great importance for highly efficient OLEDs, and it should meet some basic requirements: (a) sufficiently high triplet energy (E_T) for ensuring exothermic energy transfer from the host material to the dopant and efficient exciton confinement,[4] (b) a high morphological stability (especially, a high glass transition temperature (T_g)), (c) suitable energy level match-ups with adjacent layers to reduce interfacial energy barriers,[5] and (d) decent charge carrier transport properties to increase the opportunity for electron and hole recombination within the emitting layer.[6]

For OLEDs, if only one type of charge carrier is preferentially injected and transported, recombination of the opposite charges will be shifted out of the emissive layer, lowering the device efficiency.[7] Therefore, bipolar hosts have attracted considerable interest in the area of OLEDs because they can provide more balance in electron and hole fluxes and help increase the probability of carrier recombination.[8] A simple and viable strategy for designing bipolar hosts is to simultaneously incorporate electron donor (D) and electron acceptor (A) subunits in one molecular skeleton without lowering the E_T resulting from intramolecular charge transfer.[6] In this case, the introduction of a twisted molecular conformation may be an efficient strategy to achieve high triplet energy.

The dimer of *N*-phenyl-1-naphthylamine, N^1-(naphthalen-1-yl)-N^1,N^4-diphenylnaphthalene-1,4-diamine (**NPNA2**) has been

State Key Laboratory of Coordination Chemistry, Collaborative Innovation Center of Advanced Microstructures, School of Chemistry and Chemical Engineering, Nanjing University, Nanjing 210093, P. R. China. E-mail: yxzheng@nju.edu.cn

† Electronic supplementary information (ESI) available. See DOI: 10.1039/c5nj00939a

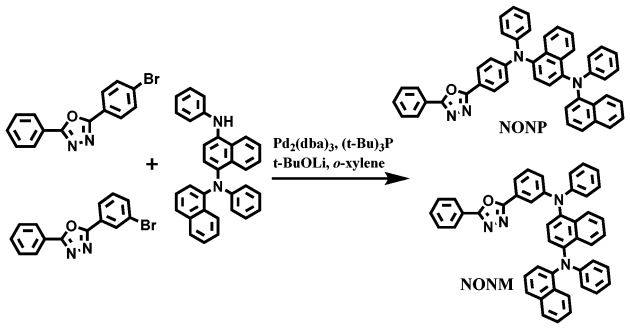

Scheme 1 Synthetic routes of **NONP** and **NONM**.

characterized to have high triplet energy, excellent hole-transporting ability and high thermal stability.[9] The 1,3,4-oxadiazole (**OXD**) derivatives are well established electron-transporting and hole-blocking materials used in OLEDs due to the electron-withdrawing nature of this aromatic heterocycle molecule.[10] In this study, the hole-transporting **NPNA2** and electron-transporting 1,3,4-oxadiazole moieties were selected for the construction of two new bipolar compounds (Scheme 1), N^1-(naphthalen-1-yl)-N^1,N^4-diphenyl-N^4-(4-(5-phenyl-1,3,4-oxadiazol-2-yl)phenyl) naphthalene-1,4-diamine (**NONP**) and N^1-(naphthalen-1-yl)-N^1,N^4-diphenyl-N^4-(3-(5-phenyl-1,3,4-oxadiazol-2-yl)phenyl) naphthalene-1,4-diamine (**NONM**), to study the effects of the positions of 1,3,4-oxadiazole on the phenyl bridge. As the yellow phosphors play the indispensable role in achieving high efficiencies in two-color, all-phosphor white organic light-emitting diodes, the yellow phosphor Ir(bt)$_2$(acac) (bis(2-phenylbenzothiozolato-N,$C^{2\prime}$)iridium(acetylacetonate))[11] was chosen as emitter in this study. In our previous report, we fabricated devices with hosts connecting triphenylsilane, **NPNA2** moieties and Ir(bt)$_2$(acac) as guest, which achieved a maximum current efficiency of 40.8 cd A^{-1}.[12] Unfortunately, those materials are hole transport hosts. Therefore, we introduce the more electron-deficient moiety **OXD** to develop the bipolar property of the hosts and expect to achieve higher efficiencies of PHOLEDs. The triplet energy levels of the two novel host materials are higher than Ir(bt)$_2$(acac), and efficient energy transfer from the host materials to the Ir(bt)$_2$(acac) is expected.

Results and discussion

Synthesis and thermal property

Scheme 1 shows the synthetic routes and structures of **NONP** and **NONM**. The starting materials, 2-(4-bromophenyl)-5-phenyl-1,3,4-oxadiazole and 2-(3-bromophenyl)-5-phenyl-1,3,4-oxadiazole, were synthesized from the ring-closing reaction of *N*-benzoyl-4-bromobenzohydrazide and *N*-benzoyl-4-bromobenzo hydrazide, respectively, which were prepared by hydrazinolysis of benzoyl chloride. N^1-(naphthalen-1-yl)-N^1,N^4-diphenyl naphthalene-1,4-diamine (**NPNA2**) was synthesized as reported previously.[9] Buchwald-Hartwig crossing-coupling of 2-(4-bromophenyl)-5-phenyl-1,3,4-oxadiazole and 2-(3-bromophenyl)-5-phenyl-1,3,4-oxadiazole with **NPNA2** gave **NONP** and **NONM** with yields higher than 60%.

The thermal properties of **NONP** and **NONM** were characterized by thermogravimetric analysis (TGA, Fig. 1) and differential scanning calorimetry (DSC, Fig. 1). TGA of **NONP** and **NONM** showed a decomposition temperature (T_d) corresponding to 5% weight loss as high as 424 °C and 375 °C, respectively. More importantly, high glass transition temperatures are observed in **NONP** (T_g = 127 °C) and **NONM** (T_g = 106 °C). This can be partly due to the molecular structures contained in the hole-transporting unit **NPNA2**, which increase molecular asymmetry and molecular weight. This demonstrated that the two host materials are capable of forming uniform amorphous films, one of the key factors for highly efficient PHOLEDs.

Photophysical properties

Photophysical properties of **NONP** and **NONM** were examined by UV-vis and photoluminescence (PL) spectrometry (Fig. 2 and Table 1). The absorption spectra of **NONP**, **NONM** and Ir(bt)$_2$(acac) were tested in dichloromethane solution. The two short-wavelength absorptions peaking at 268 and 276 nm in **NONP** and **NONM** can be attributed to the π–π* transitions from the electron-donating **NPNA2** moiety to the electron-accepting **OXD** unit (intramolecular charge transfer). The longer-wavelength absorptions observed at 351 nm for **NONP** and 372 nm for **NONM** are attributed to the **NPNA2**-centered n–π* transition. The absorption bands of (bt)$_2$Ir(acac) at 441 and 481 nm belong to the absorption transition from ground state to singlet ^{1}MLCT and triplet ^{3}MLCT excited states.[13]

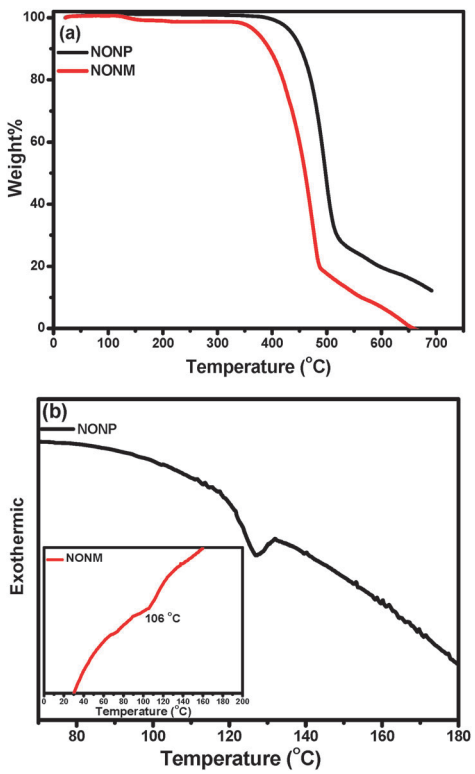

Fig. 1 TGA (a) and DSC (b) thermograms of **NONP** (black line) and **NONM** (red line).

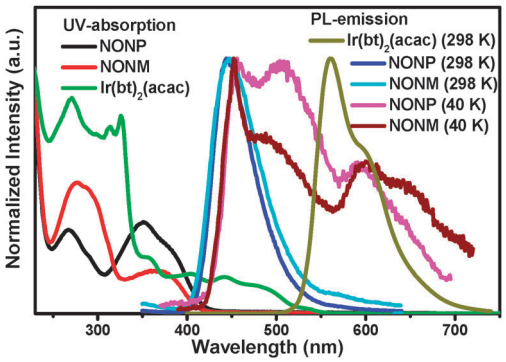

Fig. 2 UV-vis spectra of **NONP**, **NONM** and $Ir(bt)_2(acac)$ in dichloromethane solution at room temperature; photoluminescence spectra of **NONP**, **NONM** and $Ir(bt)_2(acac)$ in dichloromethane solution at 298 K; phosphorescence spectra of **NONP** and **NONM** at 40 K.

The fluorescence spectra of **NONP** and **NONM** and the phosphorescence spectrum of $Ir(bt)_2(acac)$ at room temperature are also shown in Fig. 2. The maximum emission peak of $Ir(bt)_2(acac)$ is located at 560 nm with a slight shoulder at 597 nm. The emission peaks of **NONP** and **NONM** at room temperature are 444 and 447 nm, respectively. There is a good overlap between the emission bands of **NONP** and **NONM** and the MLCT absorption of $Ir(bt)_2(acac)$, suggesting a possible energy transfer from **NONP** and **NONM** to $Ir(bt)_2(acac)$, which can be confirmed by the emission spectra of $Ir(bt)_2(acac)$ doped in **NONP** and **NONM** dichloromethane solutions with different doping concentrations (Fig. S1, ESI†). The triplet state lifetimes (τ) for the two hosts are in millisecond scale at 40 K (Table 1, Fig. S2, ESI†). Low-temperature PL measurement was detected at 40 K (Fig. 2) to calculate the triplet energies of the **NONP** and **NONM** as 2.71 and 2.73 eV, respectively (Table 1). These energies are higher than the triplet energy of the common yellow phosphorescent dopant $Ir(bt)_2(acac)$ (E_T = 2.2 eV).[14] Hence, **NONP** and **NONM** can be appropriate hosts for $Ir(bt)_2(acac)$, and carriers can be well confined in the emissive layers.

To gain insight into the geometric and electric properties of the compounds, quantum chemistry calculation was performed using the TDDFT/B3LYP/6-31G(d**) method.[15] As shown in Fig. 3, their HOMOs (highest occupied molecular orbitals) are localized predominantly on the electron-rich **NPNA2** unit and the attached buffer unit of benzene, and the LUMOs (lowest unoccupied molecular orbitals) are localized predominantly on electron-deficient **OXD** fragments. And, having minor differences in electronic properties, the photoluminescent features between the two hosts were also similar. Compared with the slight overlap between HOMO and LUMO for **NONP**, **NONM** has almost complete separation of the HOMO and LUMO due to the steric effects in *meta*-linkage through the benzene unit. The two host materials both have potential to show bipolar property, which is an important factor for enhancing the efficiency and lowering the operating voltage of PHOLEDs.[16]

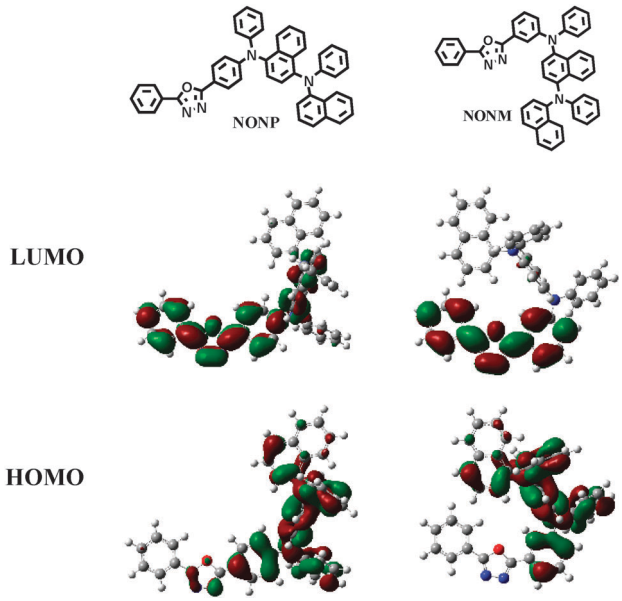

Fig. 3 Spatial distributions of the HOMO and LUMO levels for **NONP** and **NONM**.

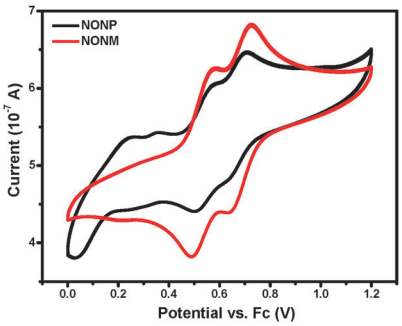

Fig. 4 Cyclic voltammograms of **NONP** and **NONM** in dichloromethane solution with 0.1 M $TBAPF_6$ as supporting electrolyte.

Cyclic voltammetry (CV) was performed to study the electrochemical property of **NONP** and **NONM**. Fig. 4 shows that both compounds have two reversible reduction and oxidation behaviors, indicating good electrochemical stability and the potential to have bipolar carrier-transporting property.[17] The HOMO energy levels of the two compounds were calculated

Table 1 Photophysical data of compounds **NONP** and **NONM**

Compound	T_d/T_g[a] (°C)	Absorption λ_{abs}[b] (nm)	Emission λ_{em}[b] (nm)	E_T[c] (eV)	τ[d] (ms)	HOMO (eV)	LUMO (eV)
NONP	424/127	268/351	444	2.71	1.2, 13.9	−5.27	−2.33
NONM	375/105	276/372	447	2.73	1.04, 14.8	−5.25	−2.30

[a] T_g: glass transition temperature, T_d: decomposition temperature. [b] Measured in dichloromethane solution at 298 K. [c] Triplet energy: estimated from the highest-energy peaks of the 40 K phosphorescence spectra. [d] Measured in zeonex at 40 K, λ_{ex} = 380 nm.

from onset potentials of oxidation as −5.27 and −5.25 eV for **NONP** and **NONM**, respectively, by comparing with ferrocene (Fc) (HOMO = $-(E_{ox} + 4.8)$ eV). The corresponding LUMO levels calculated from the HOMO values and the band gaps (estimated to be 2.94 and 2.95 eV from the edge of UV-vis absorption) were found to be approximately −2.33 (**NONP**) and −2.30 eV (**NONM**), respectively. Thus, theoretically low hole and electron injection barriers between the widely used hole-transporting layer (1,1-bis[4-(di-*p*-tolylamino)phenyl]cyclohexane) (TAPC, −5.50/−2.0 eV)[18] or the electron-transporting layer 1,3,5-tri(*m*-pyrid-3-yl-phenyl)-benzene (TmPyPB, −6.68/−2.73 eV)[19] and the hosts can be realized.

OLED performance

The charge-transporting property of the two compounds was investigated by fabricating hole-only and electron-only devices. The hole-only devices (**HODs**) have the configuration of ITO (indium tin oxide)/host (30 nm)/TAPC (60 nm)/Al (100 nm), while the electron-only devices (**EODs**) have the configuration of ITO/TmPyPB (60 nm)/host (30 nm)/LiF (1 nm)/Al (100 nm). A TAPC or TmPyPB layer was used to prevent electron or hole injection from the cathode or anode, respectively. We also fabricated TAPC-only and TmPyPB-only devices. The current density *versus* voltage curves for these devices are shown in Fig. 5. As the current densities of TAPC and TmPyPB are much larger than **HODs** and **EODs**, the effect of TAPC and TmPyPB on charge transport can be neglected. In **HODs** and **EODs**, both **NONP** and **NONM**-based devices showed a smaller difference in current density between **HODs** and **EODs**. This indicates that the two compounds are capable of transporting holes and electrons, and they exhibit bipolar character by the introduction of the hole transport unit **NPNA2** and the electron-drawing moiety **OXD**. The hole and electron current densities of **NONM** were slightly higher than those of **NONP**, which indicates that **NONM** shows better performance than **NONP** in terms of charge transport. This can be attributed to the asymmetric substitution at the *meta* position, which is an effective strategy for the design of high-performance bipolar host materials.[17]

The electroluminescence (EL) performance of the bipolar host materials **NONP** and **NONM** were evaluated with devices having the common structure ITO/TAPC (40 nm)/ host: $Ir(bt)_2(acac)$ (15 wt%, 20 nm)/TmPyPB (40 nm)/LiF (1 nm)/Al (100 nm).

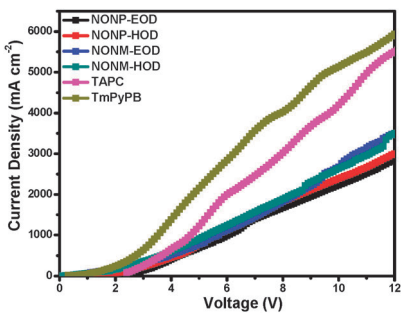

Fig. 5 Current density *versus* voltage for the hole-only (**HOD**) and the electron-only (**EOD**) devices.

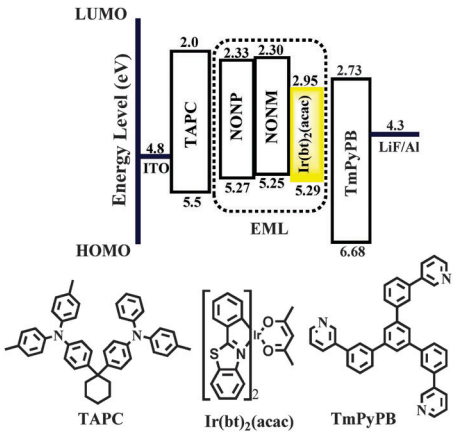

Fig. 6 Energy level diagram of yellow PHOLEDs and molecular structures of materials used.

The molecule structures and energy level diagrams of the materials and devices are shown in Fig. 6. TAPC and TmPyPB were used as the hole- and electron-transporting layers, respectively. $Ir(bt)_2(acac)$ was used as the phosphor emitter with the optimized doping concentration of 15 wt%, which is a little higher than common yellow devices.[20] This is because more electrons were trapped directly at the dopant molecules at higher doping level due to the low LUMO level of $Ir(bt)_2(acac)$, which provided an additional channel for electron transport through hopping between the dopant sites.[21] Accordingly, a higher dopant concentration, such as 15 wt%, improved the charge balance and energy transfer from host to guest.[22]

The EL spectra of the **NONP**- and **NONM**-based yellow PHOLEDs showed a main peak at 562 nm and a slight shoulder peak at 595 nm from $Ir(bt)_2(acac)$ (Fig. 7); both devices emit yellow light with Commission Internationale de l'Eclairage (CIE) color coordinates of (0.49, 0.51). This means that the host materials undergo highly efficient exothermic energy transfer from the host to dopant in the emitting layer upon electrical excitation. Additionally, no other emission bands were observed in the devices, which is partly due to the well-balanced charge density in the emission zone.[22]

As shown in Fig. 8a, the current density–voltage–luminance (*J*–*V*–*L*) characteristic curves of the **NONP**- and **NONM**-based devices demonstrate that the turn-on voltage is only 2.7 V. One important reason for such low turn-on voltage is the bipolar

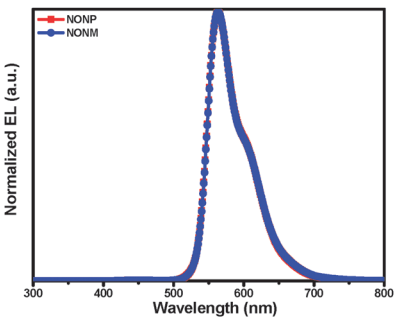

Fig. 7 EL spectra of **NONP**- and **NONM**-based yellow PHOLEDs.

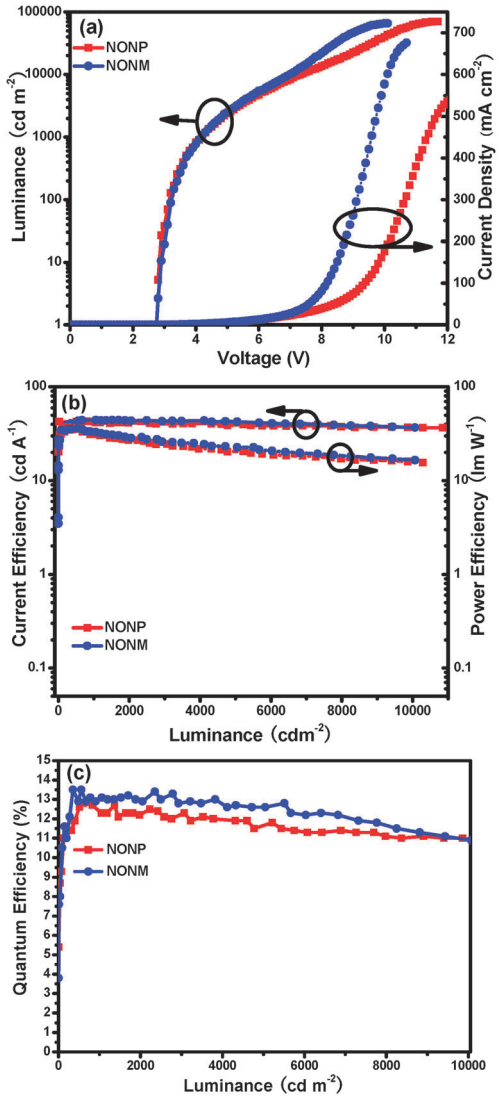

Fig. 8 (a) Current density–voltage–luminance (*J*–*V*–*L*), (b) current efficiency–luminance (η_c–*L*) and power efficiency–luminance (η_p–*L*), and (c) external quantum efficiency–luminance (EQE–*L*) characteristics of the PHOLEDs with **NONP** and **NONM**.

transporting property of the hosts. Another reason is the suitable HOMO and LUMO energy levels of the two hosts, which better match the work function of the hole-transporting layer TAPC and the electron-transporting layer TmPyPB, improving the charge injection of the device. The current density of the yellow PHOLED with **NONM** as the host was higher than that of the yellow PHOLED with **NONP** as the host, which is in agreement with the current density–voltage curves of the **HODs** and **EODs** shown in Fig. 5.

All the devices show good performance for emission in the yellow region, better than our previous results using silane-based hole transport host materials.[9] Furthermore, the device using *para*-linked host **NONP** achieves a maximum current efficiency ($\eta_{c,max}$) of 43.2 cd A^{-1}, a maximum power efficiency ($\eta_{p,max}$) of 35.7 lm W^{-1} and a maximum external quantum efficiency (EQE) of 12.9% with a maximum luminance of 70 156 cd m^{-2} at 11.7 V (Table 2). In comparison, the device using *meta*-linked **NONM** as host exhibits slightly higher efficiencies with a $\eta_{c,max}$ of 44.4 cd A^{-1}, a $\eta_{p,max}$ of 35.9 lm W^{-1}, an EQE of 13.5% and a maximum brightness of 65 737 cd m^{-2} at 10.1 V, which can be elucidated from the following two aspects. First, the compound **NONM** appears to have a better balance of electron- and hole-transporting properties than that of compound **NONP**, which may result in balanced charge densities and a broad distribution of recombination regions within the emitting layer. Second, the slightly higher triplet energy of **NONM** (2.73 eV) could more efficiently suppress adverse energy back-transfer from the $Ir(bt)_2(acac)$ to the host than that of **NONP** (2.71 eV), consequently resulting in better performance. This result also proved that the efficiencies were improved by only changing the position of the substituents.

It is worth mentioning that the current efficiency roll-off ratios for both devices are mild. For example, at the luminance of 3000 cd m^{-2}, the current efficiency values of **NONP**- and **NONM**-based devices are still as high as 40.4 and 43.6 cd A^{-1}, respectively. This can be attributed to the balanced charge density and efficient exciton recombination in the broad area of the emitting zone.[23]

Conclusions

Two new bipolar materials, **NONP** and **NONM**, comprising the hole-transporting unit N^1-(naphthalen-1-yl)-N^1,N^4-diphenylnaphthalene-1,4-diamine and the electron-transporting moiety 1,3,4-oxadiazole, were successfully synthesized. Both materials showed sufficiently high triplet energy, good thermal ability and balanced charge mobility. Used as hosts for yellow PHOLEDs with low efficiency roll-off, the device bearing *meta*-linked **NONM** performed with a maximum current efficiency of 44.4 cd A^{-1}, a maximum power efficiency of 35.9 lm W^{-1}, a maximum external quantum efficiency of 13.5%, and a maximum luminance of 70 156 cd m^{-2} – a little higher than that of the *para*-linked host **NONP**-based device, which showed a

Table 2 Electroluminescence performance of the devices based on **NONP** and **NONM**

Host	$V_{turn\text{-}on}$[a] (V)	L_{max} (voltage)[b] [cd m^{-2} (V)]	$\eta_{c,max}$ (luminance)[c] [cd A^{-1} (cd m^{-2})]	$\eta_{c,L3000}$[d] [cd A^{-1}]	$\eta_{p,max}$ (luminance)[e] [lm W^{-1} (cd m^{-2})]	EQE_{max}[f] [%]	CIE[g] [*x*, *y*]
NONP	2.7	70 156 (11.7)	43.2 (612)	40.4	35.7 (612)	12.9	0.49, 0.51
NONM	2.7	65 737 (10.1)	44.4 (1703)	43.6	35.9 (556)	13.5	0.49, 0.51

[a] $V_{turn\text{-}on}$: turn-on voltage recorded at a luminance of 1 cd m^{-2}. [b] L_{max}: maximum luminance. [c] $\eta_{c,max}$: maximum current efficiency. [d] $\eta_{c,L3000}$: current efficiency at 3000 cd m^{-2}. [e] $\eta_{p,max}$: maximum power efficiency. [f] EQE_{max}: maximum external quantum efficiency. [g] Measured at 8 V.

maximum current efficiency of 44.4 cd A^{-1}, a maximum power efficiency of 35.9 lm W^{-1}, a maximum external quantum efficiency of 13.5%, and a maximum brightness of 65 737 cd m^{-2}. These results indicate that this work provides a way to design ideal host materials for yellow PHOLEDs.

Experimental

Materials and measurements

^{1}H NMR and ^{13}C NMR spectra were measured on a Bruker AM 500 spectrometer. Mass spectra (MS) were obtained with MALDI-TOF (Bruker Daltonic Inc.). High-resolution electrospray ionisation mass spectra (HR ESI-MS, Agilent 6540 UHD Accurate-Mass Q-TOF LC/MS) were recorded for the compounds. TGA and DSC measurements were carried out on the STA 449F3 (NETZSCH) and 823e (METTLER), respectively. Absorption and emission spectra were measured on a Shimadzu UV-3100 and a Hitachi F-4600 luminescence spectrophotometer, respectively. The low-temperature phosphorescence spectra were measured with an Edinburgh Instruments FLS-920 spectrophotometer at 40 K. Cyclic voltammetric experiments were carried out with CHI 600E system (Chenhua, Shanghai) using three-electrode cell assemblies in de-aerated dichloromethane solution with tetrabutylammoniumperchlorate as supporting electrolyte and at a scan rate of 100 mV s^{-1}. Each oxidation potential was calibrated using ferrocene as reference.

OLED fabrication and measurement

Organic chemicals used for OLEDs were generally purified by high-vacuum, temperature gradient sublimation. The devices were fabricated by vacuum deposition of the materials at 10^{-6} Torr onto an ITO glass substrate (a sheet resistance of 15 Ω square^{-1}) with a deposition rate of 1–2 Å s^{-1}. The phosphor and host were co-evaporated to form a 20 nm emitting layer from two separate sources. The LiF and Al were deposited with deposition rates of 0.1 and 3 Å s^{-1}, respectively. The characteristics of the devices were measured with a computer-controlled KEITHLEY 2400 source meter with a calibrated silicon diode in air without device encapsulation. The CIE coordinates were calculated using a testing program of the Spectra scan PR650 spectrophotometer.

Syntheses

All reactions were performed under nitrogen. Solvents were carefully dried and distilled from appropriate drying agents prior to use for the synthesis of ligands. **NPNA2** was synthesized according to our previous report.[9]

2-(4-Bromophenyl)-5-phenyl-1,3,4-oxadiazole. Benzoyl chloride (5 mmol, 0.70 g) was added dropwise to a solution of 4-bromobenzoyl hydrazine (5 mmol, 1.08 g) and triethylamine (5 mmol, 0.50 g) in chloroform (8 mL) at room temperature. The resulting mixture was stirred for 1 h and then filtered. The collected solid was washed with water and ethanol to give the product *N*-benzoyl-4-bromobenzohydrazide (1.51 g, yield: 95%). A mixture of *N*-benzoyl-4-bromobenzo-hydrazide (1.51 g) and $POCl_3$ (15 mL) in a 100 mL flask was refluxed under nitrogen for 5 h. The excess $POCl_3$ was then distilled out, and the residue was poured into water. The crude product was collected by filtration and purified by recrystallization from chloroform/hexane to give white, needle-like crystals (1.21 g, yield: 85%). ^{1}H NMR (500 MHz, $CDCl_3$) δ 8.18–8.16 (m, 1H), 8.16 (s, 1H), 8.04 (d, J = 8.5 Hz, 2H), 7.71 (d, J = 8.5 Hz, 2H), 7.57 (td, J = 8.7, 4.9 Hz, 3H). MALDI-TOF MS (FAB, m/z) calcd for $C_{14}H_9BrN_2O$: 299.990. Found: 300.458 $[M]^+$.

2-(3-Bromophenyl)-5-phenyl-1,3,4-oxadiazole. 2-(3-Bromophenyl)-5-phenyl-1,3,4-oxadiazole was prepared according to the same procedure as compound 2-(4-bromophenyl)-5-phenyl-1,3,4-oxadiazole, but 3-bromobenzoyl hydrazine instead of 4-bromobenzoyl hydrazine was used as a starting material. ^{1}H NMR (500 MHz, $CDCl_3$) δ 8.31 (d, J = 1.3 Hz, 1H), 8.20–8.15 (m, 2H), 8.12 (dd, J = 7.8, 0.9 Hz, 1H), 7.72 (dd, J = 8.0, 0.9 Hz, 1H), 7.61–7.55 (m, 3H), 7.45 (t, J = 7.9 Hz, 1H). MALDI-TOF MS (FAB, m/z) calcd for $C_{14}H_9BrN_2O$: 299.990. Found: 300.479 $[M]^+$.

***N*^{1}-(Naphthalen-1-yl)-*N*^{1},*N*^{4}-diphenyl-*N*^{4}-(4-(5-phenyl-1,3,4-oxadiazol-2-yl)phenyl)naphthalene-1,4-diamine (NONP).** $Pd_2(dba)_3$ (0.09 g, 0.10 mmol), **NPNA2** (0.04 g, 1.0 mmol), Li^{t}BuO (0.32 g, 4.0 mmol) and 2-(4-bromophenyl)-5-phenyl-1,3,4-oxadiazole (0.36 g, 1.2 mmol) were added into a 50 mL two-neck flask. The flask was evacuated and backfilled with nitrogen. *O*-xylene (20 mL) and P^{t}Bu$_3$ (1.23 mL, 0.4 mmol, 10% in *n*-hexane) were injected. The mixture was heated at 140 °C for 48 h and extracted twice with CH_2Cl_2 at room temperature. The mixed organic solution was washed with brine, and the solid obtained was purified with column chromatography on SiO_2 using ethyl acetate and petroleum ether (v : v = 1 : 50) as eluant to afford a yellowish solid **NONP** (67%). ^{1}H NMR (500 MHz, $CDCl_3$) δ 8.12 (ddd, J = 19.7, 16.7, 8.5 Hz, 4H), 7.95 (td, J = 13.6, 8.1 Hz, 4H), 7.75 (d, J = 8.3 Hz, 1H), 7.54 (dd, J = 10.9, 4.7 Hz, 3H), 7.50 (d, J = 7.1 Hz, 1H), 7.41 (ddd, J = 15.8, 12.2, 7.6 Hz, 4H), 7.35–7.30 (m, 4H), 7.21–7.16 (m, 3H), 7.14–7.09 (m, 2H), 7.03 (d, J = 8.9 Hz, 2H), 6.93 (t, J = 7.3 Hz, 2H), 6.80 (d, J = 8.0 Hz, 2H). ^{13}C NMR (126 MHz, $CDCl_3$) δ[ppm] 164.71, 163.91, 151.52, 150.35, 146.75, 144.68, 144.08, 139.44, 135.29, 132.48, 131.64, 131.42, 130.27, 129.55, 129.06, 129.02, 128.55, 128.16, 127.84, 126.93, 126.78, 126.65, 126.34, 126.13, 125.92, 125.28, 125.21, 125.13, 124.43, 124.32, 124.22, 124.08, 123.95, 120.99, 120.58, 119.04, 115.27. HR ESI-MS (m/z) calcd for $C_{46}H_{32}N_4O$: 657.2649. Found: 657.2650 $[M + 1]^+$.

***N*^{1}-(Naphthalen-1-yl)-*N*^{1},*N*^{4}-diphenyl-*N*^{4}-(3-(5-phenyl-1,3,4-oxadiazol-2-yl)phenyl)naphthalene-1,4-diamine (NONM).** Compound **NONM** was prepared according to the same procedure as compound **NONP**, but 2-(3-bromophenyl)-5-phenyl-1,3,4-oxadiazole was used instead of 2-(4-bromophenyl)-5-phenyl-1,3,4-oxadiazole as a starting material with a yield of 60%. ^{1}H NMR (500 MHz, $CDCl_3$) δ 8.14 (d, J = 8.5 Hz, 1H), 8.10 (dd, J = 6.7, 1.6 Hz, 3H), 8.03 (d, J = 8.1 Hz, 1H), 7.91 (d, J = 8.4 Hz, 1H), 7.86–7.84 (m, 1H), 7.74 (d, J = 8.2 Hz, 1H), 7.69 (d, J = 7.7 Hz, 1H), 7.59–7.51 (m, 3H), 7.48 (d, J = 8.1 Hz, 2H), 7.43–7.30 (m, 7H), 7.19–7.09 (m, 6H), 7.04 (t, J = 7.3 Hz,2H), 6.91 (t, J = 7.3 Hz, 1H), 6.80 (d, J = 7.4 Hz, 2H). ^{13}C NMR (126 MHz, $CDCl_3$) δ[ppm] 150.37, 149.28, 147.68, 144.67, 143.68, 140.10,

135.26, 132.54, 131.66, 130.24, 129.96, 129.43, 129.04, 128.51, 127.65, 126.94, 126.76, 126.56, 126.30, 126.15, 126.08, 125.83, 125.27, 125.18, 125.08, 124.85, 124.60, 124.37, 124.22, 123.96, 122.78, 122.56, 120.84, 120.47, 119.71, 118.91. HR ESI-MS (*m*/*z*) calcd for $C_{46}H_{32}N_4O$: 657.2649. Found: 657.2627 $[M + 1]^+$.

Acknowledgements

This work was supported by the National Natural Science Foundation of China (21371093, 91433113), the Major State Basic Research Development Program (2011CB808704, 2013CB922101) and the Natural Science Foundation of Jiangsu Province (BK20130054).

Notes and references

1 E. Mondal, W.-Y. Hung, H.-C. Dai, H.-F. Chen, P.-Y. Hung and K.-T. Wong, *Tetrahedron*, 2014, **70**, 6328.

2 (*a*) F.-M. Hsu, C.-H. Chien, P.-I. Shih and C.-F. Shu, *Chem. Mater.*, 2009, **21**, 1017; (*b*) M. A. Baldo, C. Adachi and S. R. Forrest, *Phys. Rev. B: Condens. Matter Mater. Phys.*, 2000, **62**, 10967; (*c*) X. Xu, X. Yang, J. Dang, G. Zhou, Y. Wu, H. Li and W.-Y. Wong, *Chem. Commun.*, 2014, **50**, 2473; (*d*) X. Yang, G. Zhou and W.-Y. Wong, *J. Mater. Chem. C*, 2014, **2**, 1760.

3 (*a*) S.-J. Su, H. Sasabe, T. I. Takeda and J. Kido, *Chem. Mater.*, 2008, **20**, 1691; (*b*) B. H. Zhang, G. P. Tan, C.-S. Lam, B. Yao, C.-L. Ho, L. H. Liu, Z. Y. Xie, W.-Y. Wong, J. Q. Ding and L. X. Wang, *Adv. Mater.*, 2012, **24**, 1873.

4 M. Sudhakar, P. I. Djurovich, T. E. Hogen-Esch and M. E. Thompson, *J. Am. Chem. Soc.*, 2003, **125**, 7796.

5 (*a*) J. S. Swensen, E. Polikarpov, A. V. Ruden, L. Wang, L. S. Sapochak and A. B. Padmaperuma, *Adv. Mater.*, 2011, **21**, 3250; (*b*) K. Goushi, R. Kwong, J. J. Brown, H. Sasabe and C. Adachi, *J. Appl. Phys.*, 2004, **95**, 7798; (*c*) Q. Wang, I. W. H. Oswald, M. R. Perez, H. P. Jia, A. A. Shahub, Q. Q. Qiao, B. E. Gnade and M. A. Omary, *Adv. Funct. Mater.*, 2014, **24**, 4746; (*d*) Q. Wang, I. W. H. Oswald, M. R. Perez, H. P. Jia, B. E. Gnade and M. A. Omary, *Adv. Funct. Mater.*, 2013, **23**, 5420; (*e*) Q. Wang, I. W. H. Oswald, X. L. Yang, G. J. Zhou, H. P. Jia, Q. Q. Qiao, Y. H. Chen, J. Hoshikawa-Halbert and B. E. Gnade, *Adv. Mater.*, 2014, **26**, 8107.

6 (*a*) Y. T. Tao, C. L. Yang and J. G. Qin, *Chem. Soc. Rev.*, 2011, **40**, 2943; (*b*) Y. T. Tao, Q. Wang, C. L. Yang, Q. Wang, Z. Q. Zhang, T. T. Zou, J. G. Qin and D. G. Ma, *Angew. Chem., Int. Ed.*, 2008, **120**, 8224; (*c*) H. H. Chou and C. H. Cheng, *Adv. Mater.*, 2010, **22**, 2468; (*d*) S. L. Gong, Q. Fu, Q. Wang, C. L. Yang, C. Zhong, J. G. Qin and D. G. Ma, *Adv. Mater.*, 2011, **23**, 4956; (*e*) M. S. Lin, L. C. Chi, H. W. Chang, Y. H. Huang, K. C. Tien, C. C. Chen, C. H. Chang, C. C. Wu, A. Chaskar, S. H. Chou, H. C. Ting, K. T. Wong, Y. H. Liu and Y. Chi, *J. Mater. Chem.*, 2012, **22**, 870; (*f*) H. F. Chen, T. C. Wang, W. Y. Hung, H. C. Chiu, C. Yun and K. T. Wong, *J. Mater. Chem.*, 2012, **22**, 9658; (*g*) E. Mondal, W. Y. Hung, H. C. Dai and K. T. Wong, *Adv. Funct. Mater.*, 2013, **23**, 3096; (*h*) H. C. Ting, Y. M. Chen, H. W. You, W. Y. Hung, S. H. Lin, A. Chaskar, S. H. Chou, Y. Chi, R. H. Liu and K. T. Wong, *J. Mater. Chem.*, 2012, **22**, 8399; (*i*) H. F. Chen, T. C. Wang, S. W. Lin, W. Y. Hung, H. C. Dai, H. C. Chiu, K. T. Wong, M. H. Ho, T. Y. Cho, C. W. Chen and C. C. Lee, *J. Mater. Chem.*, 2012, **22**, 15620; (*j*) H. F. Chen, L. C. Chi, W. Y. Hung, W. J. Chen, T. Y. Hwu, Y. H. Chen, S. H. Chou, E. Mondal, Y. H. Liu and K. T. Wong, *Org. Electron.*, 2012, **13**, 2671; (*k*) S. J. Su, C. Cai and J. Kido, *J. Mater. Chem.*, 2012, **22**, 3447.

7 F. Dumur and F. Goubard, *New J. Chem.*, 2014, **38**, 2204.

8 Y.-L. Liao, C.-Y. Lin, K.-T. Wong, T.-H. Hou and W.-Y. Hung, *Org. Lett.*, 2007, **9**, 4511.

9 S. Zhang, L.-S. Xue, Y.-M. Jing, X. Liu, G.-Z. Lu, X. Liang, H.-Y. Li, Y.-X. Zheng and J.-L. Zuo, *Dyes Pigm.*, 2015, **118**, 1.

10 S.-H. Cheng, S.-H. Chou, W.-Y. Hung, H.-W. You, Y.-M. Chen, A. Chaskar, Y.-H. Liu and K.-T. Wong, *Org. Electron.*, 2013, **14**, 1086.

11 T. Giridhar, W. Cho, Y.-H. Kim, T.-H. Han, T.-W. Lee and S.-H. Jin, *J. Mater. Chem. C*, 2014, **2**, 9398.

12 S. Zhang, Q.-L. Xu, Y.-M. Jing, X. Liu, G.-Z. Lu, X. Liang, Y.-X. Zheng and J.-L. Zuo, *RSC Adv.*, 2015, **5**, 27235.

13 (*a*) X. Wei, J. Peng, J. Cheng, M. Xie, Z. Lu, C. Li and Y. Cao, *Adv. Funct. Mater.*, 2007, **17**, 3319; (*b*) S. M. Chen, G. P. Tan, W.-Y. Wong and H.-S. Kwok, *Adv. Funct. Mater.*, 2011, **21**, 3785.

14 B. H. Zhang, G. P. Tan, C.-S. Lam, B. Yao, C.-L. Ho, L. H. Liu, Z. Y. Xie, W.-Y. Wong, J. Q. Ding and L. X. Wang, *Adv. Mater.*, 2012, **24**, 1873.

15 A. D. Becke, *J. Chem. Phys.*, 1993, **98**, 5648.

16 (*a*) C. Fan, F. Zhao, P. Gan, S. Yang, T. Liu, C. Zhong, D. Ma, J. Qin and C. Yang, *Chem. – Eur. J.*, 2012, **18**, 5510; (*b*) C. Han, Y. Zhao, H. Xu, J. Chen, Z. Deng, D. Ma, Q. Li and P. Yan, *Chem. – Eur. J.*, 2011, **17**, 5800.

17 (*a*) Y. T. Tao, Q. Wang, C. L. Yang, Q. Wang, Z. Q. Zhang, T. T. Zou, J. G. Qin and D. G Ma, *Angew. Chem., Int. Ed.*, 2008, **47**, 8104; (*b*) Y.-L. Liao, C.-Y. Lin, K.-T. Wong, T.-H. Hou and W.-Y. Hung, *Org. Lett.*, 2007, **9**, 4511; (*c*) Y. Shirota and H. Kageyama, *Chem. Rev.*, 2007, **107**, 953; (*d*) C.-J. Zheng, J. Ye, M.-F. Lo, M.-K. Fung, X.-M. Ou, X.-H. Zhang and C.-S. Lee, *Chem. Mater.*, 2012, **24**, 643.

18 G. Liaptsis and K. Meerholz, *Adv. Funct. Mater.*, 2013, **23**, 359.

19 J.-K. Bin, N.-S. Cho and J.-I. Hong, *Adv. Mater.*, 2012, **24**, 2911.

20 H.-F. Chen, T.-C. Wang, S.-W. Lin, W.-Y. Hung, H.-C. Dai, H.-C. Chiu, K.-T. Wong, M.-H. Ho, T.-Y. Cho, C.-W. Chen and C.-C. Lee, *J. Mater. Chem.*, 2012, **22**, 15620.

21 F.-M. Hsu, C.-H. Chien, P.-I. Shih and C.-F. Shu, *Chem. Mater.*, 2009, **21**, 1017.

22 S. Zhang, Q.-L. Xu, Y.-M. Jing, X. Liu, G.-Z. Lu, X. Liang, Y.-X. Zheng and J.-L. Zuo, *RSC Adv.*, 2015, **5**, 27235.

23 M. J. Cho, S. J. Kim, S. H. Yoon, J. Shin, T. R. Hong, H. J. Kim, Y. H. Son, J. S. Kang, H. A. Um, T. W. Lee, J.-K. Bin, B. S. Lee, J. H. Yang, G. S. Chae, J. H. Kwon and D. H. Choi, *ACS Appl. Mater. Interfaces*, 2014, **6**, 19808.